The composition of magnetite in Archean mafic-ultramafic intrusions within the Superior Province

A.-A. Sappin* and M.G. Houlé

Geological Survey of Canada, 490 rue de la Couronne, Québec, Quebec G1K 9A9
*Corresponding author's e-mail: anne-aurelie.sappin@canada.ca

ABSTRACT

The mineral chemistry of magnetite from eleven Archean mafic, mafic-ultramafic, and ultramafic intrusions within the Superior Province was determined to be used as a petrogenetic indicator and to identify the most prospective areas for exploration of Fe-Ti-V and Fe-Ti-P mineralization.

The composition of magnetite is influenced by the presence of exsolutions and inclusions (e.g. ilmenite, Al-spinel), the type of parental melt (e.g. komatiitic, basaltic) and its Ti contents (e.g. high-Ti or low-Ti parental magmas), and the element partitioning with co-crystallized minerals (e.g. clinopyroxene) or previously crystallized minerals (e.g. chromite). The overall composition of magnetite, however, appears to be mainly independent of the host-rock type. The composition of magnetite in compatible (e.g. Mg, Co, V, Ni, and Cr) and incompatible (e.g. Al, Ga, Mn, Ti, Zn) elements during fractionation processes also provides useful information about the degree of differentiation of the host intrusions. Among the studied intrusions with a mafic-dominated composition, the Rivière Bell and Lac Doré complexes appear to be the most evolved, whereas the Croal Lake, Big Mac, Butler, and Wabassi Main intrusions and the Highbank-Fishtrap intrusive complex are the most primitive. Furthermore, the variation of the minor and trace element contents of the magnetite could be used to determine the internal stratigraphy within the mafic to ultramafic intrusions. For example, in the mafic-dominated Big Mac intrusion and in the ultramafic-dominated Baie Chapus Pyroxenite, the more vent-proximal facies appear to be located to the north and to the east, respectively. In addition, the V and Ni+Cr contents of magnetite from the Big Mac intrusion suggest that the northern part of this intrusion is a prospective area for Fe-Ti-V mineralization, whereas the southern part has more potential for Fe-Ti-P mineralization. In the Baie Chapus Pyroxenite, the concentrations in V and Ni+Cr in magnetite support the prospectivity of this intrusion for Fe-Ti-V mineralization.

Magnetite from the oxide-bearing mafic to ultramafic rocks and the semi-massive to massive Fe-Ti oxide layers have lower Ti+V values than expected, with magnetite compositions plotting within the fields for hydrothermal deposits in Ni/(Cr+Mn) versus Ti+V, Ca+Al+Mn versus Ti+V, and Ni+Cr versus Ti+V discrimination diagrams. Considering that the Fe-Ti-V deposit fields in these diagrams were mostly defined based on Fe-oxides hosted within Proterozoic and Phanerozoic Fe-Ti deposits, the preliminary results presented here suggest there may be a specific signature for magnetite from Archean Fe-Ti-V-oxide-bearing intrusions. However, further work is required to confirm this distinct signature to the Archean.

INTRODUCTION

The concentration of minor and trace elements in Fe-oxides is controlled by their environment of formation, which makes magnetite a useful petrogenetic tracer and a suitable indicator mineral for mineral exploration (e.g. Dare et al., 2012, 2014). Ultramafic and mafic intrusions/flows are generally prospective units to host orthomagmatic ore deposits and are ubiquitous throughout the Superior Province, although their abundance is variable across the Province and only a limited number of these units host economic Ni-Cu-(PGE) or Fe-Ti-V-P deposits.

In this contribution, we report magnetite composition from 11 Mesoarchean to Neoarchean, mafic to ultramafic intrusions (i.e. Mayville, Croal Lake, Big Mac, Eagle's Nest, Butler, Highbank-Fishtrap, Oxtoby Lake, Wabassi Main, Baie Chapus, Rivière Bell, and Lac Doré) across the Bird River–Uchi–Oxford-Stull–La Grande Rivière–Eastmain (BUOGE "superdomain") domains and the Wawa-Abitibi terrane within the Superior Province (Fig. 1). The characterization of the minor and trace element contents of magnetite from each intrusion provided information about the factors that controlled the composition of this mineral, the degree of fractionation, and the internal stratigraphy of each intrusion, as well as information about the potential use of magnetite as a prospectivity indicator for Fe-Ti-V-P mineralization and the validity of magnetite discrimination diagrams to determine the mineral deposit environment in which these Fe-oxide grains formed (e.g. Dupuis and Beaudoin, 2011).

Sappin, A.-A. and Houlé, M.G., 2020. The composition of magnetite in Archean mafic-ultramafic intrusions within the Superior Province; *in* Targeted Geoscience Initiative 5: Advances in the understanding of Canadian Ni-Cu-PGE and Cr ore systems – Examples from the Midcontinent Rift, the Circum-Superior Belt, the Archean Superior Province, and Cordilleran Alaskan-type intrusions, (ed.) W. Bleeker and M.G. Houlé; Geological Survey of Canada, Open File 8722, p. 181–196. https://doi.org/10.4095/326896

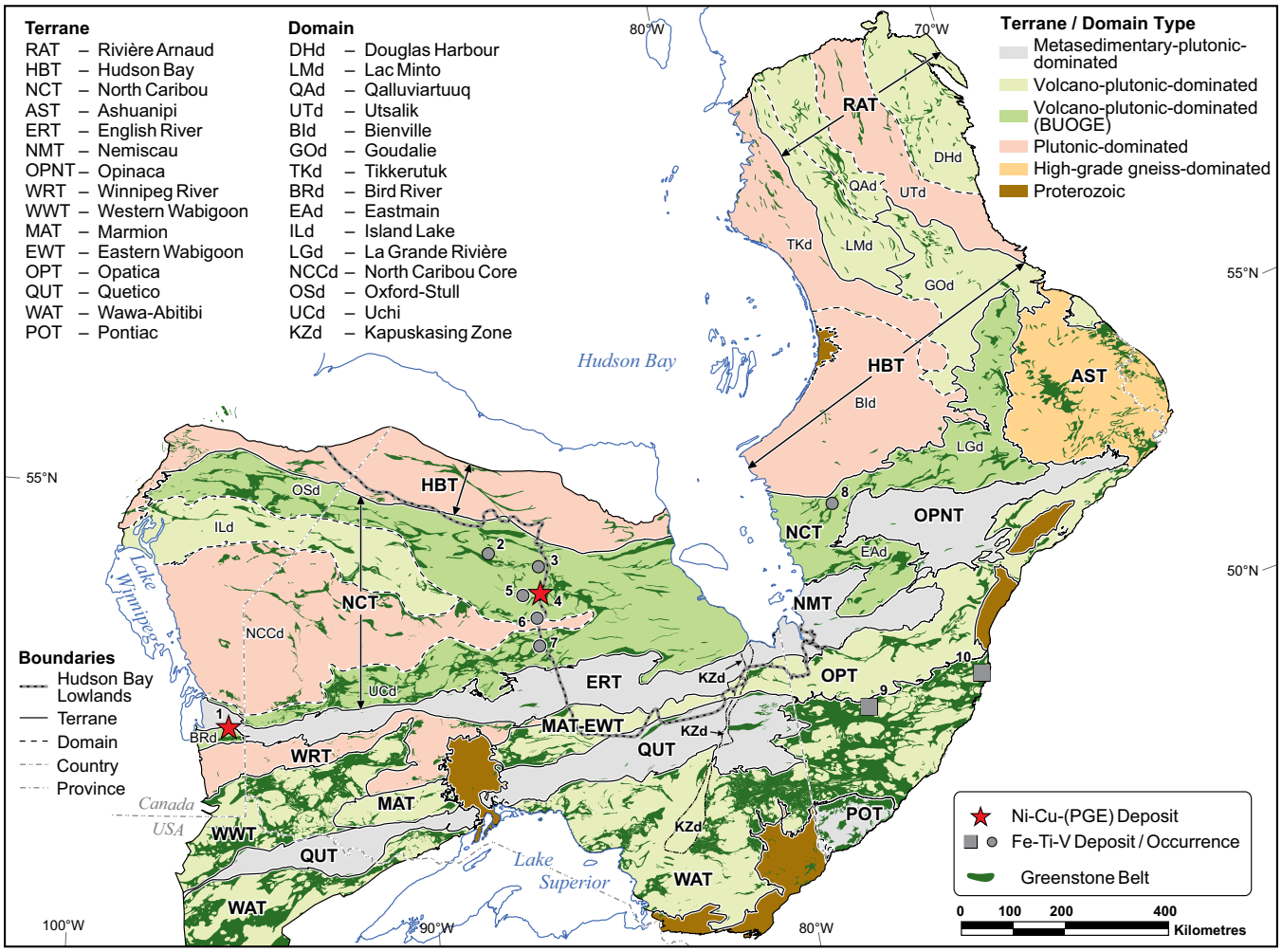

Figure 1. Geological map showing the locations of the mafic to ultramafic intrusions that were studied across the Bird River–Uchi–Oxford-Stull–La Grande Rivière–Eastmain (BUOGE) domains and the Wawa-Abitibi terrane (*after* Houlé et al., 2020). Terrane and domain boundaries are *modified from* Stott et al. (2010), Percival et al. (2012), and SIGÉOM (2020). Names of the host intrusions of the deposits/occurrences: 1 = Mayville intrusion, 2 = Croal Lake intrusion, 3 = Big Mac intrusion, 4 = Eagle's Nest dyke, 5 = Butler West and East intrusions, 6 = Highbank-Fishtrap intrusive complex, 7 = Oxtoby Lake and Wabassi Main intrusions, 8 = Baie Chapus Pyroxenite, 9 = Rivière Bell complex, 10 = Lac Doré complex.

SAMPLING AND METHODOLOGY

Sampling

A total of 83 representative drill core or grab samples were collected from 11 mafic to ultramafic intrusions across the Superior Province: the Mayville intrusion (n=2) of the Bird River intrusive suite within the Bird River domain in the North Caribou terrane (Manitoba); the Croal Lake (n=10), Big Mac (n=17), Eagle's Nest (n=1), and Butler (n=3) intrusions from the Ring of Fire intrusive suite and the Highbank-Fishtrap intrusive complex (n=19) within the Oxford-Stull domain in the North Caribou terrane (Ontario); the Oxtoby Lake (n=3) and Wabassi Main (n=11) intrusions within the Uchi domain in the North Caribou terrane (Ontario); the Baie Chapus Pyroxenite (n=11) within the La Grande Rivière domain in the North Caribou terrane (Quebec); and the Rivière Bell (n=5) and Lac Doré (n=1) complexes within the Abitibi greenstone belt in the Wawa-Abitibi terrane (Quebec) (Fig. 1, Table 1, 2). A total of 727 magnetite grains from 83 samples were analyzed by electron probe micro-analyzer (EPMA) and 240 magnetite grains from 36 samples were analyzed using laser ablation-inductively coupled plasma mass spectrometry (LA-ICP-MS) (Table 2).

Methodology

Minor and trace element contents of magnetite (Mg, V, Ni, Cr, Al, Mn, Ti, Zn, and Ca) were determined by EPMA at the Université Laval (Québec, Canada), using a method modified from Boutroy et al. (2014). Mg, Co, V, Ni, Cr, Al, Ga, Mn, Ti, Zn, and Ca were also determined by LA-ICP-MS spot analysis at the Geological Survey of Canada (Ottawa, Canada). The LA-ICP-MS analyses of magnetite included the ilmenite exsolutions formed during subsolidus exsolution-oxidation processes. However, the EPMA analyses of the mag-

Table 1. Summary of the main characteristics of the studied mafic to ultramafic intrusions across the Superior Province.

Intrusive Unit	Terrane/Domain	Magmatic Suite		Mineralization	Age	MF/UM Ratio	Lithology	Parental Magma
		Suite	Subsuite	Deposit/*Occurrence*				
Mayville intrusion	NCT - BRd	BRIS		Cu-Ni-PGE, *Cr-PGE*	ca. 2743 Ma[1]	MF >> UM	Gabbroic-anorthositic rocks, minor peridotite, pyroxenite, and chromitite layers	Basaltic[5]
Croal Lake intrusion	NCT - OSd	RoFIS	ERSS	*Fe-Ti-V*	ca. 2733 Ma[1]	MF >>> UM	Gabbroic rocks (±Ol), minor peridotite, anorthosite, and semi-massive to massive Fe-Ti oxides	-
Big Mac intrusion	NCT - OSd	RoFIS	ERSS	*Fe-Ti-V*	ca. 2734 Ma[1]	MF >>> UM	Gabbroic rocks, minor anorthosite, pyroxenite, and semi-massive to massive Fe-Ti oxides	-
Eagle's Nest dyke	NCT - OSd	RoFIS	KLSS	Ni-Cu-PGE	-	UM >>> MF	Komatiitic dunite, lherzolite, websterite, and minor gabbroic rocks	Komatiitic[6,7]
Butler West intrusion	NCT - OSd	RoFIS	ERSS	*Fe-Ti-V*	-	MF >>> UM	Gabbroic rocks, minor anorthosite, pyroxenite, and semi-massive to massive Fe-Ti oxides	Basaltic with high-Fe and Ti contents[8]
Butler East intrusion	NCT - OSd	RoFIS	ERSS	*Fe-Ti-V*	-	MF >>> UM	Gabbroic rocks, minor anorthosite, pyroxenite, and semi-massive to massive Fe-Ti oxides	Basaltic with high-Fe and Ti contents[8]
Highbank-Fishtrap intrusive complex	NCT - OSd			*Fe-Ti-V*	ca. 2808–2810 Ma[1]	MF >> UM	Gabbroic rocks, anorthosite, pyroxenite, and minor semi-massive Fe-Ti oxides	-
Oxtoby Lake intrusion	NCT - UCd			-	ca. 2717 Ma[2]	MF	Gabbroic rocks	Basaltic[2]
Wabassi Main intrusion	NCT - UCd			*Cu-Ni*	ca. 2727 Ma[2]	MF > UM	Gabbroic rocks (±Ol), anorthosite, minor peridotite	Basaltic[2]
Baie Chapus Pyroxenite	NCT - LGd			*Fe-Ti-V*	<2802 Ma[3]	UM >> MF	Clinopyroxenite (±Pl, ±Ol), minor gabbro, wehrlite, dunite, and semi-massive to massive Fe-Ti oxides	Relatively primitive, mantle-derived[9]
Rivière Bell complex	WAT			Fe-Ti-V	ca. 2725 Ma[4]	MF >>> UM	Gabbroic rocks, minor anorthosite, granophyre, pyroxenite (±Ol), and troctolite, and semi-massive to massive Fe-Ti oxides	Basaltic[10]
Lac Doré complex	WAT			Fe-Ti-V	ca. 2728 Ma[4]	MF >>> UM	Anorthosite, gabbroic rocks, diorite, tonalite, ultramafic rock, semi-massive to massive Fe-Ti oxides	Tholeiitic[11,12]

Abbreviations:
NCT = North Caribou terrane, WAT = Wawa-Abitibi terrane
BRd = Bird River domain, LGd = La Grande Rivière domain, OSd = Oxford-Stull domain, UCd = Uchi domain
BRIS = Bird River intrusive suite, RoFIS = Ring of Fire intrusive suite, ERSS = Ekwan River subsuite, KLSS = Koper Lake subsuite
MF = mafic, Ol = olivine, PGE = platinum-group elements, Pl = plagioclase, UM = ultramafic.

References:
[1]Houlé et al., 2015a; [2]Sappin et al., 2016; [3]Houlé et al., 2015b; [4]Mortensen, 1993; [5]Yang et al., 2013; [6]Mungall et al., 2010; [7]Zuccarelli et al., 2018; [8]Kuzmich, 2014; [9]Sappin et al., 2015a; [10]Maier et al., 1996; [11]Arguin et al., 2018; [12]Mathieu, 2019.

Table 2. Main compositions of magnetite (maximum values) from the studied mafic to ultramafic intrusions across the Superior Province.

Intrusive Unit	Mayville intrusion			Croal Lake intrusion			Big Mac intrusion			Eagle's Nest dyke			Butler West intrusion			Butler East intrusion		
Rock type	MF	UM	Massive sulphides	MF	UM	SM to M Fe-Ti oxides	MF	UM	SM to M Fe-Ti oxides	MF	UM	Massive sulphides	MF	UM	SM to M Fe-Ti oxides	MF	UM	SM to M Fe-Ti oxides
Mag/Ilm ratio	Mag > Ilm	Ilm > Mag	Mag > Ilm	Mag > Ilm	-	Mag > Ilm	Mag > Ilm	Mag > Ilm	Mag > Ilm	-	-	Mag >>> Ilm	Mag > Ilm	Mag > Ilm	Mag > Ilm	Mag > Ilm	Mag > Ilm	Mag > Ilm
Total of samples																		
Number of samples	0	0	2	7	No Prim Mag	3	10	1	6	0	No Prim Mag	1	1	0	0	1	1	0
Number of analyses	-	-	36	76		78	73	20	68	-		18	18	-	-	13	15	-
EPMA data (ppm)																		
Number of samples			2	7		3	10	1	6			1	1			1	1	
Number of analyses			20	61		58	63	12	50			10	10			7	7	
Mg			339	856		881	2,256	1,490	1,466			1,530	550			500	70	
V			1,604	17,584		10,331	9,319	2,830	8,653			1,830	5,250			10,870	6,300	
Ni			311	200		240	230	100	170			810	160			190	210	
Cr			231	5,360		5,665	11,077	9,530	6,568			35,190	750			520	8,390	
Al			1,272	3,864		3,820	24,494	3,932	14,713			120	1,100			600	410	
Mn			279	1,720		922	790	240	270			3,130	140			210	320	
Ti			800	12,236		6,040	14,090	1,190	3,640			790	2,380			590	1,050	
Zn			189	900		420	240	190	932			420	260			270	240	
Ca			27	170		736	450	70	40			800	60			70	50	
LA-ICP-MS data (ppm)																		
Number of samples			2	2		3	2	1	2			1	1			1	1	
Number of analyses			16	15		20	10	8	18			8	8			6	8	
Mg			294	184		2,020	1,273	721	3,188			2,345	814			1,502	952	
Co			14	65		170	71	69	56			39	30			43	34	
V			1,686	9,118		7,300	2,069	2,558	4,597			2,523	4,796			11,780	6,580	
Ni			240	189		159	119	81	99			803	68			95	84	
Cr			200	1,440		4,559	2,773	8,685	4,053			96,409	714			392	6,427	
Al			1,211	1,490		3,460	4,041	2,794	11,837			659	1,686			1,856	1,051	
Ga			27	50		49	57	49	56			25	54			53	24	
Mn			459	3,180		3,618	3,826	5,872	3,392			11,761	2,708			3,280	6,505	
Ti			2,470	107,072		129,063	150,651	124,564	151,145			1,534	67,525			70,749	96,211	
Zn			12	595		498	78	501	1,153			667	68			52	83	
Ca			109	107		105	46	26	63			1,229	47			83	3,809	

Intrusive Unit	Highbank-Fishtrap intrusive complex			Oxtoby Lake intrusion	Wabassi Main intrusion		Baie Chapus Pyroxenite			Rivière Bell complex			Lac Doré complex		
Rock type	MF	UM	SM Fe-Ti oxides	MF	MF	UM	MF	UM	SM to M Fe-Ti oxides	MF	UM	SM to M Fe-Ti oxides	MF	UM	SM to M Fe-Ti oxides
Mag/Ilm ratio	Ilm > Mag	Ilm > Mag	Mag > Ilm	Mag > Ilm	Ilm > Mag	-	Ilm > Mag	Mag > Ilm	Mag >>> Ilm	Mag > Ilm	Mag > Ilm	Mag > Ilm	Mag > Ilm	Mag > Ilm	Mag > Ilm
Total of samples															
Number of samples	11	5	3	3	11	No Prim Mag	0	7	4	0	0	5	1	0	0
Number of analyses	98	63	38	42	82		-	84	56	-	-	77	12	-	-
EPMA data (ppm)															
Number of samples	11	5	3	3	11			7	4			5	1		
Number of analyses	84	57	31	27	58			84	40			41	7		
Mg	1,090	2,623	410	230	5,476			7,850	260			6,606	90		
V	10,120	7,749	12,309	3,711	12,380			1,740	7,440			9,710	nd		
Ni	580	786	731	1,290	1,713			1,500	620			330	60		
Cr	21,900	13,869	6,014	2,020	30,714			3,680	300			760	350		
Al	2,948	2,030	3,140	2,020	54,105			1,290	140			39,626	6,850		
Mn	860	590	150	1,180	3,830			450	750			4,167	810		
Ti	65,330	28,790	3,870	53,938	123,685			1,690	49,860			128,026	15,530		
Zn	830	1,280	610	2,030	10,347			280	540			1,516	4,240		
Ca	190	540	110	214	600			4,290	320			110	100		
LA-ICP-MS data (ppm)															
Number of samples	3	1	1	2	5			No sample	2			5	1		
Number of analyses	14	6	7	15	24				16			36	5		
Mg	188	179	677	88	5,590				404			6,128	1,042		
Co	82	58	132	67	182				41			292	57		
V	8,869	3,131	8,310	3,394	15,206				6,949			9,475	1,432		
Ni	476	13	658	337	547				366			665	15		
Cr	20,616	52	3,362	1,752	14,948				32			454	318		
Al	1,195	1,771	1,682	835	30,012				550			29,559	15,208		
Ga	44	70	44	52	85				14			61	58		
Mn	1,838	1,813	2,024	289	6,404				3,812			3,692	3,761		
Ti	67,969	118,914	76,364	296	224,453				101,402			169,773	88,265		
Zn	558	492	459	163	3,685				95			1,395	11,489		
Ca	218	235	127	14	150				417			133	21		

Abbreviations: EPMA = electron probe micro-analyzer, LA-ICP-MS = laser ablation-inductively coupled plasma-mass spectrometry; M = massive, MF = mafic, SM = semi-massive, UM = ultramafic; Ilm = ilmenite, Mag = magnetite, nd = not determined, Prim = primary.

netite excluded as much as possible any inclusions or exsolutions in order to analyze a single mineral species.

The EPMA analyses were undertaken with a CAMECA SX-100 five-spectrometer electron microprobe using 15 kV accelerating voltage, a 20 nA beam current forming a 5 µm diameter beam, and counting times of 20 s on peak and 10 s on background to determine the major and minor element contents of the magnetite grains. For the minor and trace element contents, an accelerating voltage of 15 kV, a 100 nA beam current forming a 10 µm diameter beam, counting times of 40 to 80 s on peak, and a background measured on both sides for 15 to 20 s at positions free of interferences were used. Simple oxides (GEO Standard Block, from P&H Developments) and minerals (Mineral Standard Mount MINM25-53, from Astimex Scientific Limited; reference samples from Jarosewich et al., 1980) were used as calibration standards.

The LA-ICP-MS system consisted of a Photon Machine Analyte 193 nm excimer laser ablation system coupled to an Agilent Technologies 7700x ICP-MS, which was operated using a laser frequency of 10 Hz and a spot size of 40 to 69 µm. Fe was used as the internal standard (concentrations determined by EPMA in Fe-oxides or a stoichiometric value was assumed when EPMA data were not available). Certified reference materials (GSE-1G, GSD-1G, Po726) and in-house standards of natural magnetite (BC28) were used for calibration and quality control.

In this study, only the minor and trace element concentrations at levels above EPMA and LA-ICP-MS detection limits were used. A selection of data obtained using both methods is provided in Table 2.

RESULTS

Magnetite Composition from Mafic to Ultramafic Intrusions

Magnetite grains in this study are hosted by different types of rocks, such as oxide-bearing mafic to ultramafic rocks, semi-massive to massive Fe-Ti oxide layers, and massive sulphides belonging to a wide range of mafic, mafic-ultramafic, and ultramafic intrusions (Table 2). These intrusions occur in a number of terranes/domains in the Superior Province (Bird River, Oxford-Stull, Uchi, La Grande Rivière, and Wawa-Abitibi) and have varying ages (Mesoarchean versus Neoarchean) and compositions (mafic-dominated versus ultramafic-dominated) (Table 1).

Magnetite in oxide-bearing mafic to ultramafic rocks

The oxide-bearing mafic to ultramafic rock samples (<40% Fe-Ti oxides) were collected from the mafic-dominated Croal Lake, Big Mac, Butler (East and West), Highbank-Fishtrap, Oxtoby Lake, Wabassi Main, and Lac Doré intrusions and the Baie Chapus Pyroxenite, an ultramafic-dominated intrusion (Table 2). These intrusions are all Neoarchean, except for the Highbank-Fishtrap intrusive complex, which is Mesoarchean (Table 1).

The results obtained for V and Cr contents in the magnetite determined using EPMA and LA-ICP-MS are similar (Fig. 2, Table 2). However, Mg, Al, Mn, and Ti contents determined by electron microprobe are generally lower than those determined by LA-ICP-MS, whereas Ni and Zn contents are mostly higher (Fig. 2, Table 2). During fractionation, Mg, Co, V, Ni, and Cr are compatible elements in mafic magmas and Al, Mn, Ti, and Zn are incompatible (e.g. Dare et al., 2014). In the oxide-bearing mafic to ultramafic rocks, the concentration of compatible and incompatible elements in magnetite varies from intrusion to intrusion (Fig. 2). Magnetite from the Croal Lake, Big Mac, Butler, and Highbank-Fishtrap intrusions shows high Cr and locally high V contents. Magnetite from the Oxtoby Lake intrusion has low Mg contents, relatively low Cr, Al, and Mn contents, and the lowest Ti contents of the intrusions studied. Magnetite from the Wabassi Main intrusion has the highest Mg and Co contents and high V, Ni, Cr, Al, Mn, and Ti contents. Magnetite from the Lac Doré complex has low V contents, relatively low Mg and Cr contents, and the lowest Ni contents, but high Mn, Ti, and Zn contents. Pyroxenite from the Baie Chapus intrusion contains magnetite with the highest Ni contents, relatively high Mg contents, and low V, Cr, and Al contents.

Magnetite in semi-massive to massive Fe-Ti oxides

The semi-massive and massive Fe-Ti oxide samples (40–80% and >80% Fe-Ti oxides, respectively) are from the Neoarchean mafic-dominated Croal Lake, Big Mac, and Rivière Bell intrusions, the Mesoarchean mafic-dominated Highbank-Fishtrap intrusion, and the Neoarchean ultramafic-dominated Baie Chapus Pyroxenite (Table 1, 2).

EPMA and LA-ICP-MS data for magnetite show similar concentration ranges, except for elements Mn, Ti, and, locally, Mg, Cr, and Zn (Fig. 3, Table 2). The chemical signature of the magnetite from the semi-massive to massive magnetite-ilmenite layers also varies by intrusions (Fig. 3). Magnetite from the Croal Lake and Big Mac intrusions have relatively high Mg and Cr contents, whereas magnetite from the Highbank-Fishtrap intrusive complex has relatively low Mg contents but high Cr contents. In the Rivière Bell complex, the magnetite has been affected by regional and local metamorphism and most of its primary composition, with the exception of V and Cr con-

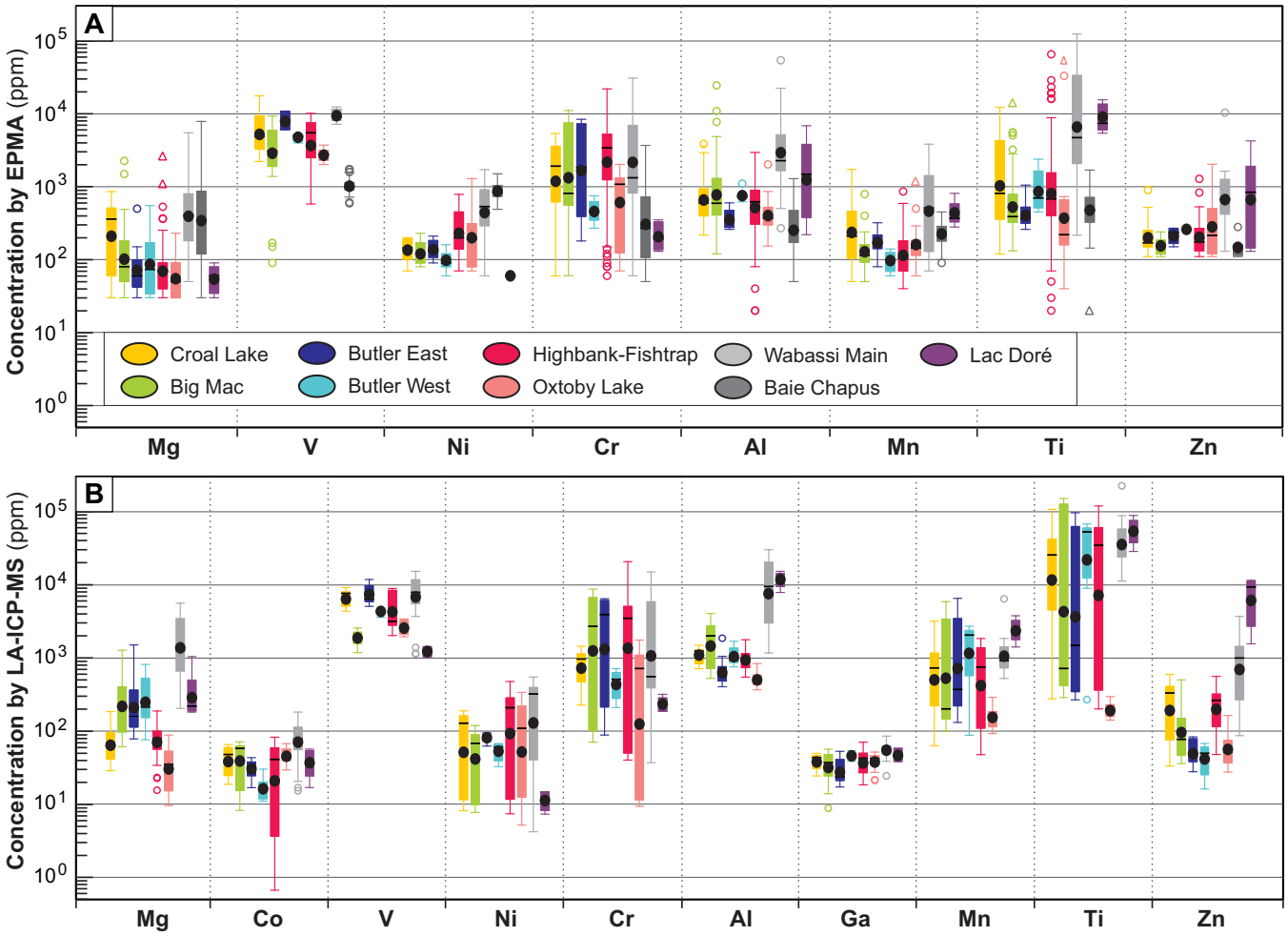

Figure 2. Box and whisker plots of selected minor and trace elements in magnetite from the Croal Lake, Big Mac, Butler (East and West), Highbank-Fishtrap, Oxtoby Lake, Wabassi Main, Baie Chapus, and Lac Doré intrusions. Magnetite in oxide-bearing mafic to ultramafic rocks were analyzed by **(a)** EPMA and **(b)** LA-ICP-MS. The upper and lower margins of the box represent the upper 75% and lower 25% of the data. The whiskers represent the upper and lower threshold values (95% of the data). Median values are shown as solid black lines and mean values as solid black circles. Outliers are shown as open circles and far outlier as open triangles along the whisker.

tents, has been modified (Polivchuk, 2017). The Fe-oxides from this complex have relatively low V and Cr contents. Semi-massive to massive Fe-Ti oxides from the Baie Chapus Pyroxenite host magnetite with intermediate Ni contents, relatively high Mn contents, locally low Mg and Zn contents, and the lowest contents of Co, Cr, Al, and Ga (an incompatible element during fractionation that is enriched in the residual liquid).

Magnetite in massive sulphides

The massive sulphide samples belong to the Neoarchean mafic-dominated Mayville and ultramafic-dominated Eagle's Nest Ni-Cu-(PGE)-bearing intrusions (Table 1, 2).

Analytical results for magnetite are similar and of the same order of magnitude, whether analyses were by EPMA or LA-ICP-MS, with the exception of results for Mn, Ti, and Zn (Fig. 4, Table 2). In general, magnetite in the Mayville intrusion contains very low concentrations of compatible elements (Mg, Co, V, and Cr; Fig. 4). In contrast, magnetite from the Eagle's Nest intrusion has higher Mg, Co, V, Ni, Cr, and Mn contents and lower Al, Ga, and Ti contents than the Mayville magnetite (Fig. 4).

Case Study: Magnetite Composition in the Big Mac Intrusion

The Big Mac mafic intrusion (ca. 2734 Ma: Houlé et al., 2015a) is part of the Ring of Fire intrusive suite within the Oxford-Stull domain (Ontario), in the central part of the Superior Province (Fig. 1). Based on geophysical data (OGS–GSC, 2011), the intrusion forms, at surface, an approximately 60 km long and 1 to 4 km wide elongate body oriented northwest-southeast (Fig. 5). It is a subconcordant sill that is broadly layered, as indicated by field observations. The Big Mac intrusion is composed of gabbro (*sensu lato*),

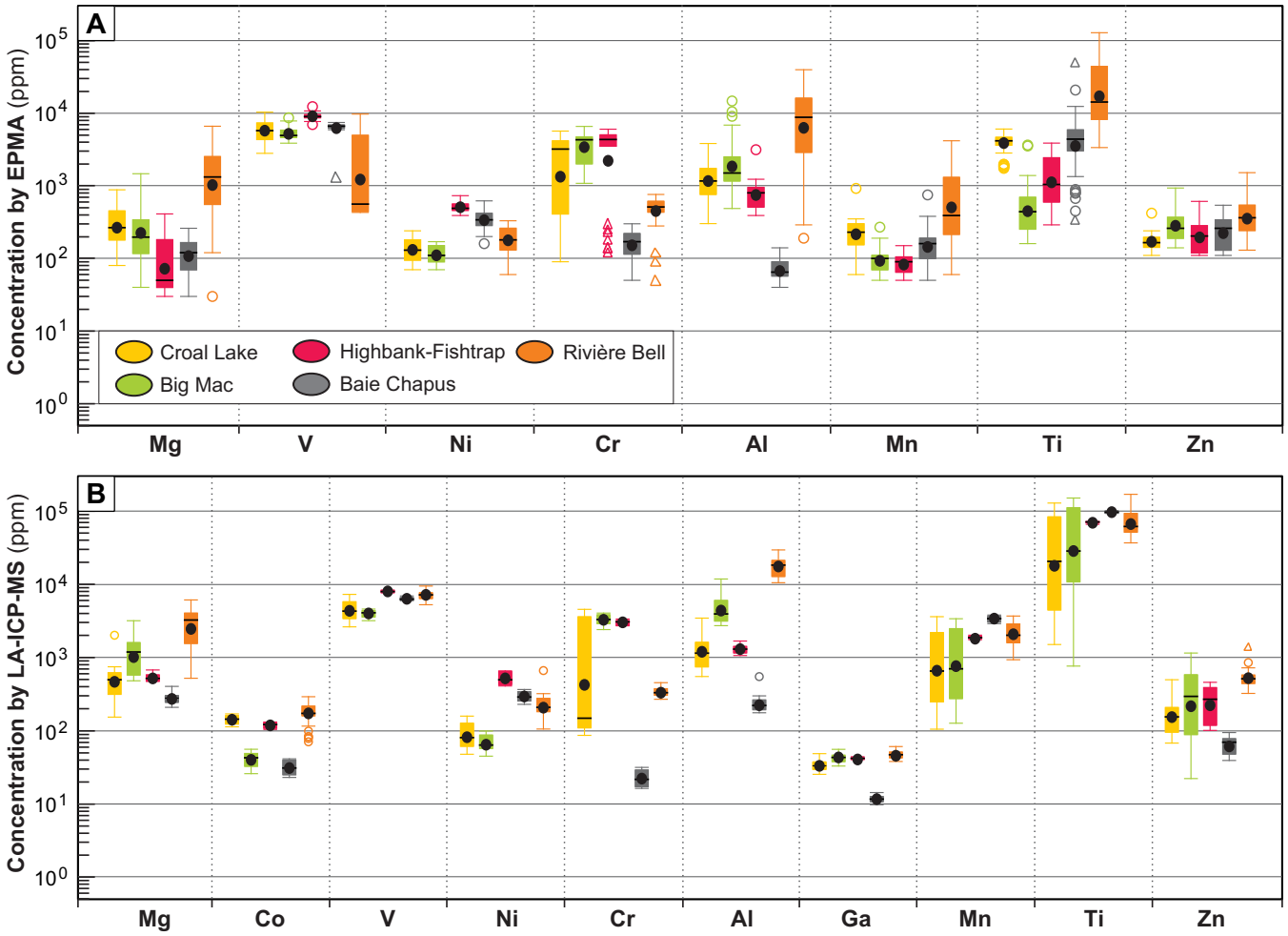

Figure 3. Box and whisker plots of selected minor and trace elements in magnetite from the Croal Lake, Big Mac, Highbank-Fishtrap, Baie Chapus, and Rivière Bell intrusions. Magnetite in semi-massive to massive Fe-Ti oxide layers were analyzed by **(a)** EPMA (a) and **(b)** LA-ICP-MS. *See* Figure 2 for the meaning of symbols in the plots.

minor anorthosite, and rare pyroxenite. It also contains a few decimetre- to metre-thick, semi-massive to massive, magnetite-ilmenite layers, which are restricted to the northern part of the intrusion.

In the Big Mac intrusion, the chemical composition of Fe-oxides varies with location. Magnetite in the northern part of the intrusion is rich in elements that are compatible in mafic magmas (i.e. Mg, V, Ni, Cr), whereas to the south, the concentration of these elements is low and it is locally rich in elements that are incompatible during fractionation process (i.e. Mn, Ti, Zn; Fig. 6). In addition, the mafic to ultramafic rocks in the northernmost part of the Big Mac intrusion have the most primitive geochemical signatures (Mg# ≤50, Cr = 2095–23 ppm, V = 1255–33 ppm, P_2O_5 = 0.14–0.03 wt%), have high magnetite/ilmenite ratios, contain plagioclase with the most primitive composition (up to An_{84}), and contain rare traces of apatite. In contrast, the southernmost part of this intrusion is characterized by mafic rocks with more evolved geochemical signatures (Mg# ≤35, Cr = 134–15 ppm, V = 453–16 ppm, P_2O_5 = 2.81–0.12 wt%), lower magnetite/ilmenite ratios, plagioclase with an evolved composition (as low as An_{25}), and up to 9 modal% apatite.

Case Study: Magnetite Composition in the Baie Chapus Pyroxenite

The Baie Chapus Pyroxenite (emplaced after 2802 Ma: Houlé et al., 2015b), is located within the La Grande Rivière domain (Quebec), in the eastern part of the Superior Province (Fig. 1). This intrusion is approximately 3 km long by 1 km wide at surface and is crudely layered, as indicated by field observations (Fig. 7). It is composed of clinopyroxenite, plagioclase clinopyroxenite, olivine clinopyroxenite, gabbro (*sensu lato*), and rare wehrlite and dunite. Significant accumulations of semi-massive to massive magnetite, which extend over at least 70 m with a thickness estimated to be a few metres, were found near the western part of the intrusion.

In the Baie Chapus Pyroxenite, the chemical composition of the magnetite also varies with location. Fe-

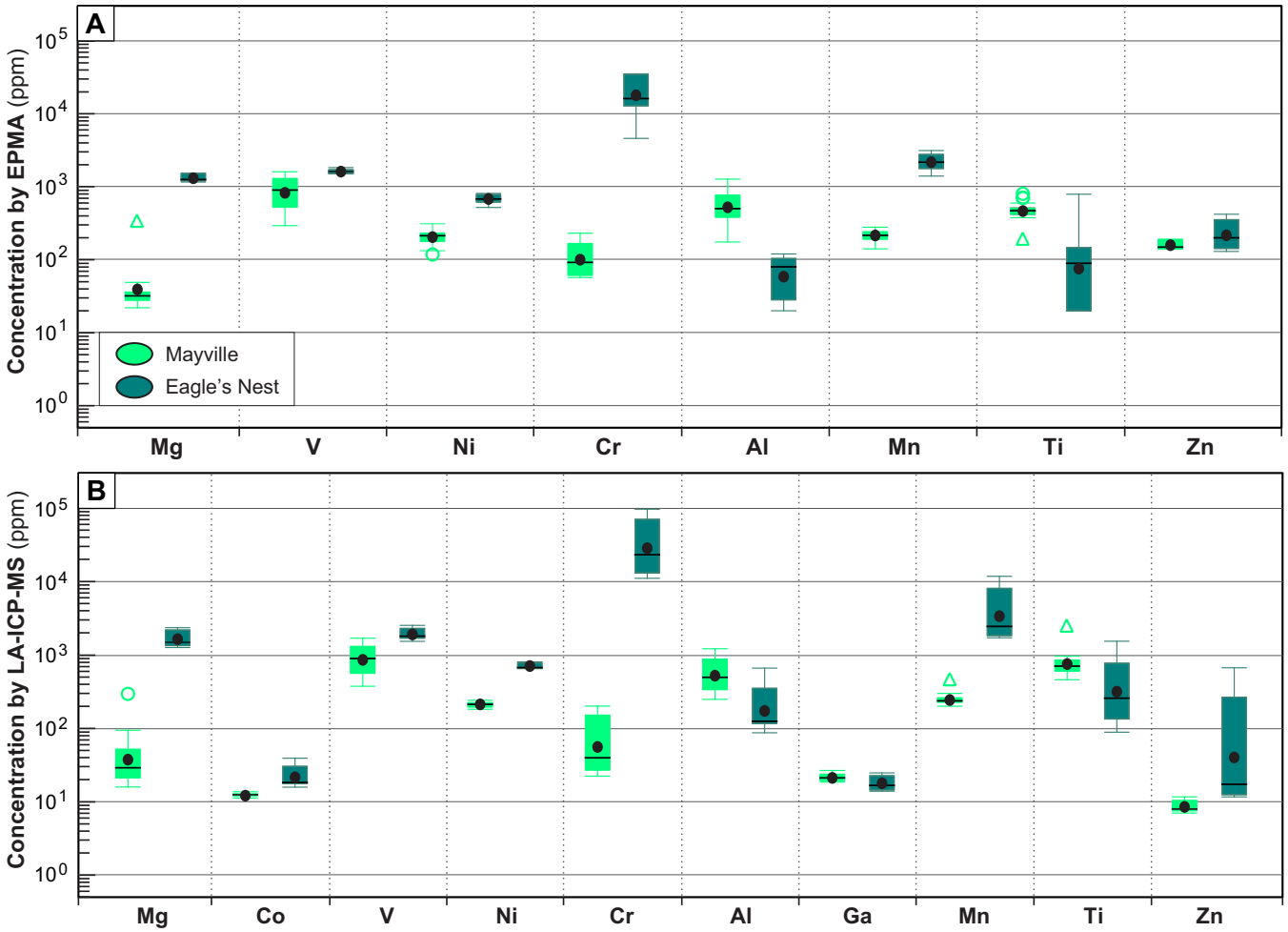

Figure 4. Box and whisker plots of selected minor and trace elements in magnetite from the Mayville and Eagle's Nest Ni-Cu-(PGE)-bearing intrusions. Magnetite in massive sulphides were analyzed by **(a)** EPMA and **(b)** LA-ICP-MS. *See* Figure 2 for the meaning of symbols in the plots.

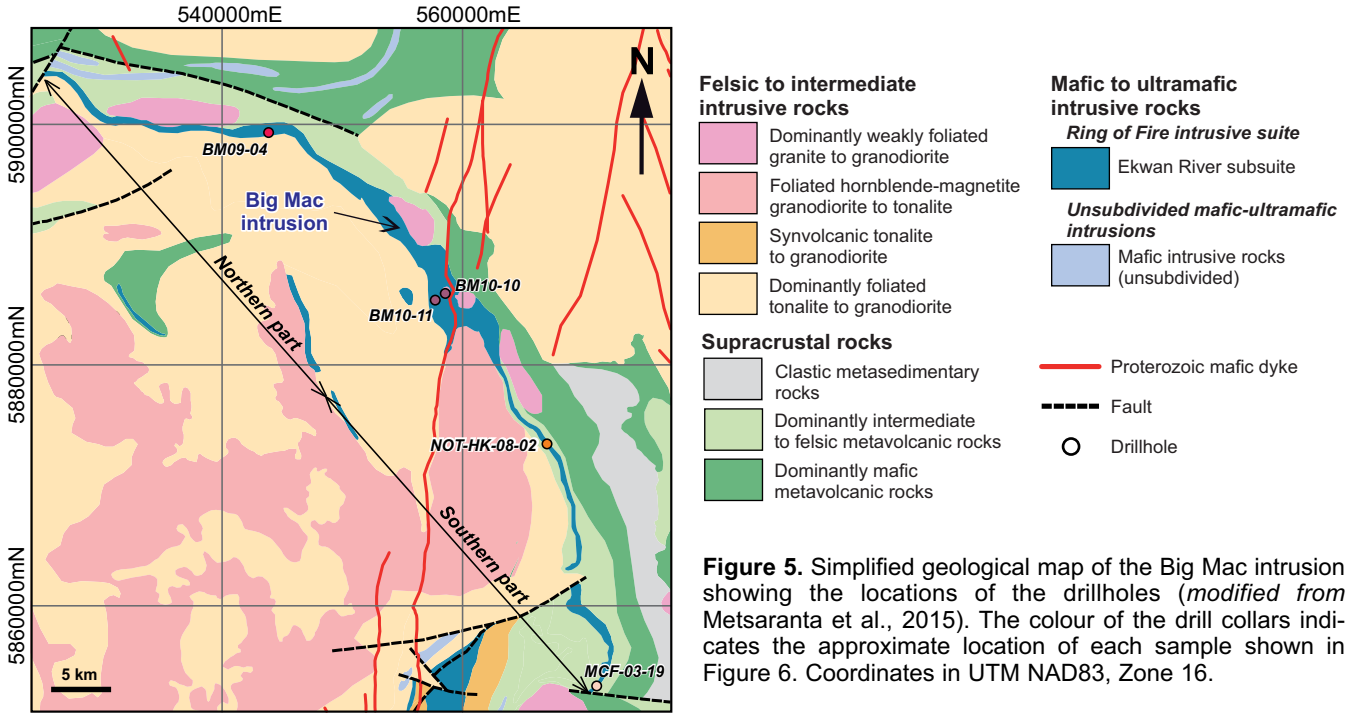

Figure 5. Simplified geological map of the Big Mac intrusion showing the locations of the drillholes (*modified from* Metsaranta et al., 2015). The colour of the drill collars indicates the approximate location of each sample shown in Figure 6. Coordinates in UTM NAD83, Zone 16.

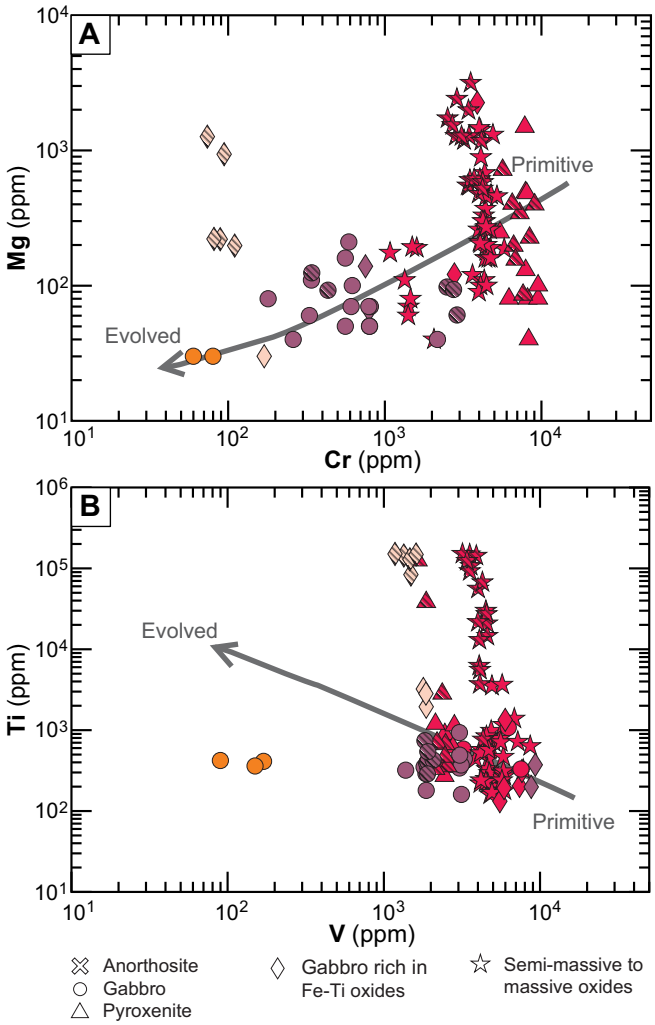

Figure 6. Composition of magnetite in anorthosite, gabbro, pyroxenite, and semi-massive to massive Fe-Ti oxide layers from the Big Mac intrusion. **a)** Mg versus Cr and **b)** Ti versus V. Each data point represents an individual magnetite grain analyzed by EPMA (nonhatched symbols) or LA-ICP-MS (hatched symbol). The fill colour of the symbols corresponds to the drill collars in Figure 5.

oxides in the eastern part of this intrusion are rich in elements that are compatible in mafic magmas, such as Mg and Cr, but to the west, the magnetite is poor in these elements and locally rich in incompatible elements (e.g. Ti, Zn) (Fig. 8a,b). Furthermore, the eastern part of the Baie Chapus Pyroxenite hosts mafic to ultramafic rocks with a relatively primitive geochemical composition (Mg# = 78–53, Cr = 703−245 ppm, V = 282−159 ppm, P_2O_5 = 0.05−0.02 wt%), clinopyroxene with a primitive composition (Mg# = 89–80), and is devoid of apatite. In contrast, the western part of this intrusion contains mafic to ultramafic rocks with a more evolved geochemical signature (Mg# = 76–41, Cr = 266−39 ppm, V = 427−41 ppm, P_2O_5 = 0.25−0.01 wt%), and up to 1 modal% apatite. Clinopyroxene in the westernmost part of this intrusion also has the most evolved composition (Mg# = 84–73).

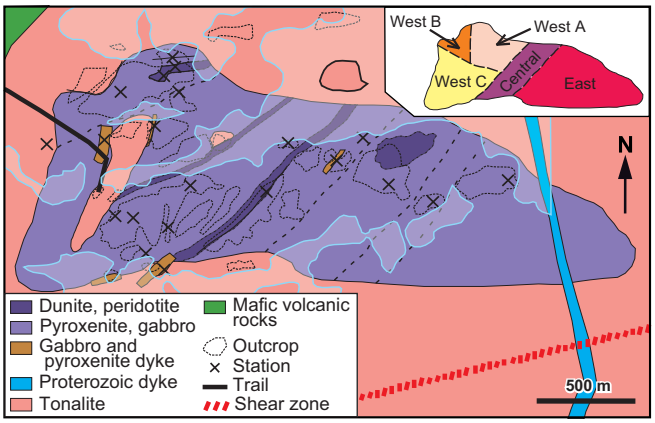

Figure 7. Simplified geological map of the Baie Chapus Pyroxenite (*modified from* Houlé and Goutier, unpubl. map). The inset indicates the different areas of this intrusion. The centre of the intrusion is approximately located at UTM (NAD83) Zone 18, 352746mE, 5928161mN.

Discrimination Diagrams of Magnetite Composition from Fe-Ti-V Deposits

Several diagrams have been proposed to classify magnetite grains based on their composition, such as the Ti versus Ni/Cr discrimination diagram for differentiating magnetite of magmatic and hydrothermal origin (Dare et al., 2014). This diagram also appears useful for identifying Ti-poor magnetite from magmatic settings (Duparc et al., 2016). The vast majority of the magnetite grains hosted by oxide-bearing mafic to ultramafic rocks and semi-massive to massive Fe-Ti oxide layers in this study have low Ni/Cr ratios, regardless of analytical method, and plot within the magmatic field of the diagram (Fig. 9). However, the magnetite from the Baie Chapus Pyroxenite, which has the highest Ni/Cr ratios, has EPMA data that plot almost entirely within the hydrothermal field (Fig. 9a). Furthermore, based on EPMA data (Fig. 9a), most of samples contain magnetite with Ti contents that are less or equal to 1 wt%. However, the LA-ICP-MS data (Fig. 9b) indicate that the Croal Lake, Big Mac, Butler, Highbank-Fishtrap, Wabassi Main, Baie Chapus, Rivière Bell, and Lac Doré intrusions host some Ti-rich magnetite (≥1 wt% Ti), whereas the Oxtoby Lake intrusion only hosts Ti-poor magnetite (mostly <0.1 wt% Ti).

Dupuis and Beaudoin (2011) defined two discrimination diagrams (Ni/(Cr+Mn) versus Ti+V and Ca+Al+Mn versus Ti+V) to distinguish magnetite associated with hydrothermal deposits (e.g. iron oxide copper-gold (IOCG) and porphyry deposits) from those associated with Fe-Ti-V deposits. In both diagrams, the field for Fe-Ti-V deposits was primarily defined based on the Fe-oxide compositions (individual grains and average compositions) determined by electron microprobe analyzer from a range of Proterozoic (General Electric mine, La Blache, and Girardville associated with Grenvillian anorthositic massif, Canada) and

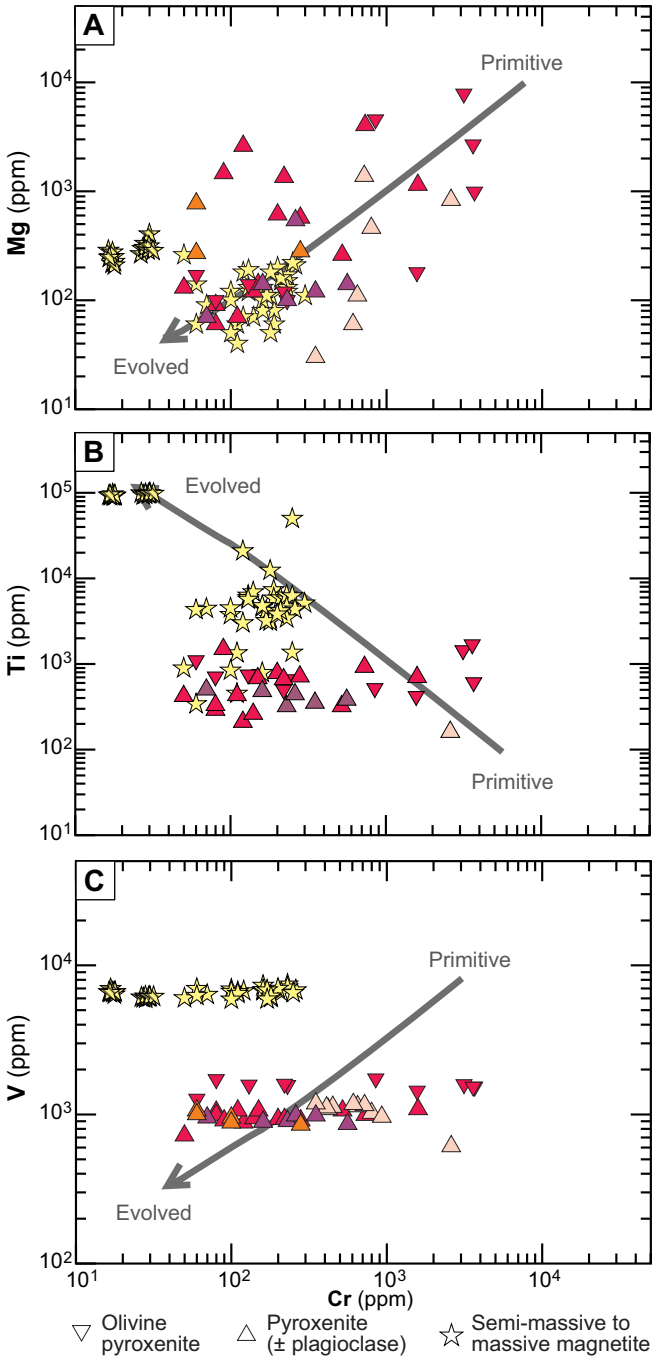

Figure 8. Composition of magnetite in pyroxenite and semi-massive to massive magnetite layers from the Baie Chapus Pyroxenite. **a)** Mg versus Cr, **b)** Ti versus Cr, and **c)** V versus Cr. Each data point represents an individual magnetite grain analyzed by EPMA (nonhatched symbols) or LA-ICP-MS (hatched symbol). The fill colour of the symbols, which corresponds to the inset map in Figure 7, indicates which area of the intrusion was sampled.

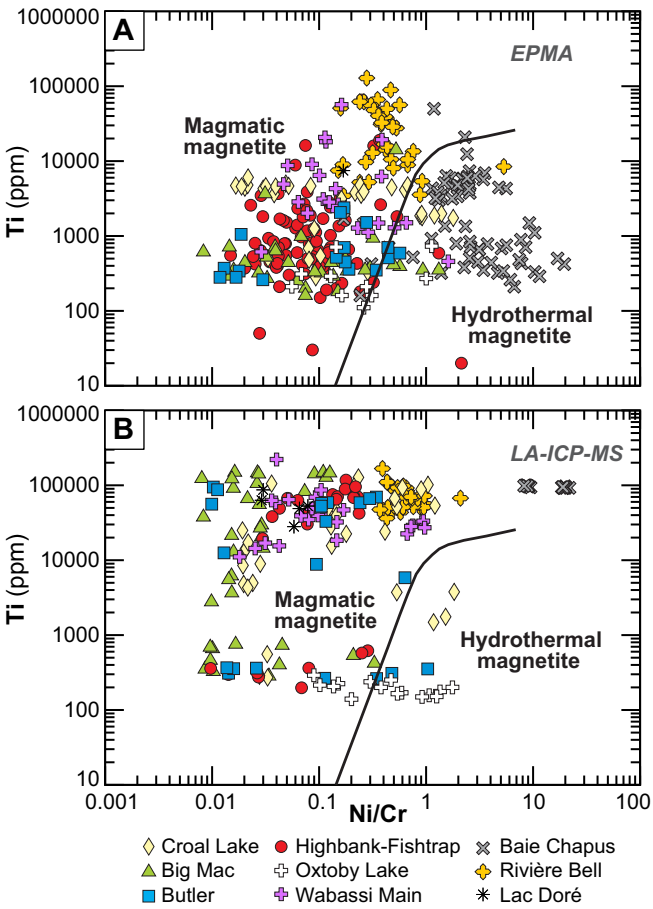

Figure 9. Ti versus Ni/Cr discrimination diagram for differentiated magmatic and hydrothermal magnetite of Dare et al. (2014) plotting magnetite from the oxide-bearing mafic to ultramafic rocks and the semi-massive to massive Fe-Ti oxide layers of the studied intrusions. **a)** Magnetite composition as determined by EPMA. **b)** Magnetite composition as determined by LA-ICP-MS. Each data point represents an individual magnetite grain.

Phanerozoic (Routivare malmfält, Sweden) Fe-Ti deposits and from the Archean Lac Doré Fe-Ti-V deposit. Méric (2011) proposed an additional Ni+Cr versus Ti+V discrimination diagram to differentiate magnetite associated with hydrothermal deposits, Fe-Ti-V deposits, and Fe-Ti-P deposits using the general Fe-Ti-V deposit field defined by Dupuis and Beaudoin (2011) for the Ni/(Cr+Mn) versus Ti+V diagram. In all these diagrams, the EPMA data for the magnetite from the oxide-bearing intrusive rocks and the semi-massive to massive Fe-Ti oxide layers of the studied Archean intrusions have significantly lower Ti+V contents than expected and plot predominantly within the field for hydrothermal deposits rather than within the field for Fe-Ti-V and Fe-Ti-P deposits (Fig. 10a,c,e). An exception is the Rivière Bell magnetite, which plots predominantly within the Fe-Ti-V deposit field (Fig. 10a,c,e). Interestingly, the LA-ICP-MS data for the magnetite grains generally plot within the Fe-Ti-V and Fe-Ti-P deposit fields in the three discrimination diagrams (Fig. 10b,d,f). However, significant LA-ICP-MS analyses from many of the intrusions of this study still plot within the hydrothermal field, in particular those for magnetite from the Oxtoby Lake intrusion (Fig. 10b,d,f), which also shows similar results when determined by EPMA (Fig. 10a,c,e).

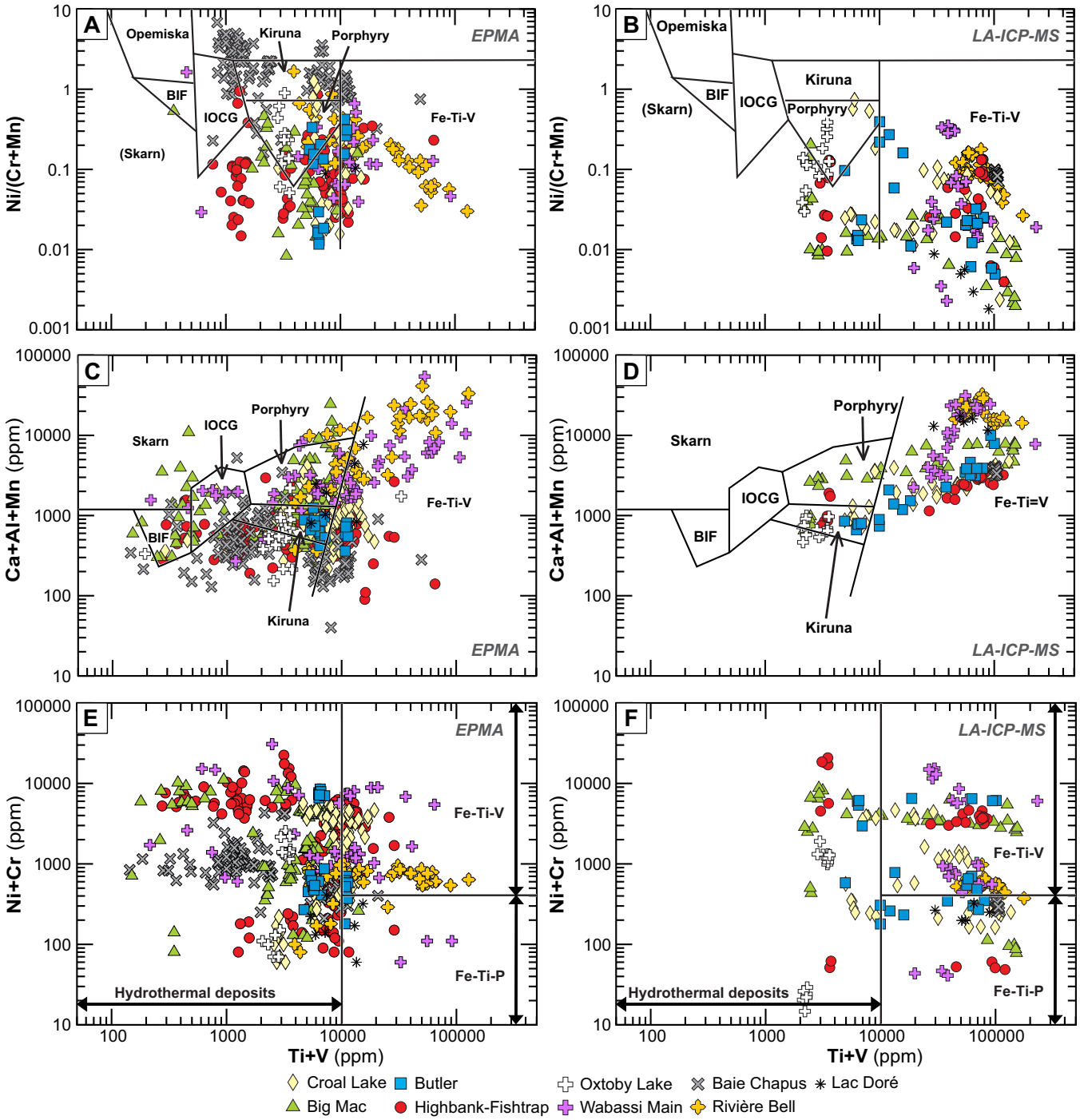

Figure 10. Discrimination diagrams of magnetite composition from hydrothermal and Fe-Ti-V deposits determined by EPMA and LA-ICP-MS. **a)** Ni/(Cr+Mn) versus Ti+V diagram for results determined by EPMA. **b)** Ni/(Cr+Mn) versus Ti+V diagram for results determined by LA-ICP-MS. **c)** Ca+Al+Mn versus Ti+V diagram for results determined by EPMA. **d)** Ca+Al+Mn versus Ti+V diagram for results determined by LA-ICP-MS. **e)** Ni+Cr versus Ti+V diagram for results determined by EPMA. **f)** Ni+Cr versus Ti+V diagram for results determined by LA-ICP-MS. Each data point represents an individual magnetite grain. Abbreviations: BIF = banded iron formation, IOCG = iron oxide copper-gold. The fields in discrimination diagrams (a), (b), (c), and (d) are from Dupuis and Beaudoin (2011), and those in (e) and (f) are from Méric (2011).

In the discrimination diagrams of Dupuis and Beaudoin (2011), Méric (2011), and Dare et al. (2014), it appears that the minor and trace element contents of magnetite from the oxide-bearing mafic and ultramafic rocks and the semi-massive to massive Fe-Ti oxide units are locally related to the type of lithology, such as in the Baie Chapus Pyroxenite (EPMA data: Fig. 9a, 10a,c,e, Table 2) and the Big Mac intrusion (EPMA and LA-ICP-MS data: Fig. 9, 10, Table 2).

DISCUSSION

Influence of the Exsolutions and/or Inclusions

Magnetite commonly contains ilmenite exsolutions that form during the subsolidus exsolution-oxidation processes (e.g. Dare et al., 2012, 2014). Unlike the electron microprobe (~5–10 µm beam size), the LA-ICP-MS uses larger beam sizes (>40 µm) that could incorporate some of these exsolutions during analyses, thus yielding a mixed analysis combining magnetite and ilmenite. However, these mixed analyses provide an estimate of the initial magnetite composition, before the Fe-oxide grains underwent subsolidus exsolutions. As a result, the EPMA and LA-ICP-MS data could show significant variations for some of the minor and trace element contents of the magnetite. For example, Ti, Mn, and Mg preferentially partition into ilmenite (Méric, 2011; Dare et al., 2014) and therefore are generally underestimated in the EPMA data (e.g. Fig. 2, 3, 9, Table 2).

The differing results for Ti contents obtained by the different analytical methods could explain the hydrothermal signature in the discrimination diagram of Dare et al. (2014) for the Baie Chapus magnetite, which was analyzed by EPMA (Fig. 9a). Indeed, LA-ICP-MS data show that these Fe-oxide grains were initially rich in Ti (>9 wt%) and plot within the magmatic field (Fig. 9b). The higher Ti contents of the Baie Chapus magnetite when determined by LA-ICP-MS could be the result of numerous Ti-enriched ilmenite exsolutions being present in the magnetite that could have been included in the LA-ICP-MS analyses but not in the EPMA results.

Other exsolutions (e.g. Al-spinel, Cr-spinel) or inclusions (e.g. sulphide) are commonly observed in magmatic magnetite (e.g. Dare et al., 2014; Huang et al., 2019). These exsolutions/inclusions could have been incorporated during LA-ICP-MS analysis, or during EPMA analysis in the case of micro- to nano-scale exsolutions/inclusions. This could explain the local variations in the minor and trace element contents of magnetite reported by the two analytical methods.

Influence of the Composition of the Parental Magma

Most of the intrusions studied that have a mafic-dominated composition (Croal Lake, Big Mac, Butler, Highbank-Fishtrap, Wabassi Main, Rivière Bell, and Lac Doré) or an ultramafic-dominated composition (Baie Chapus Pyroxenite) appear to have crystallized, at least in part, from high-Ti parental magmas. These intrusions contain some original Ti-rich magnetite (≥1 wt% Ti; Fig. 9b), suggesting that they were associated with high-Ti parental magmas. This confirms the previous results of Kuzmich (2014) about the nature of the parental magmas of the Butler intrusions (Table 1). In contrast, the low-Ti contents of the Oxtoby Lake magnetite as determined by EPMA and by LA-ICP-MS (mostly <0.1 wt% Ti, Fig. 9) indicate that these Ti-poor Fe-oxides likely crystallized from low-Ti parental magmas. It also suggests that the Ti-poor magmatic Fe-oxides could have higher Ni/Cr ratios than is predicted by the discrimination diagram of Dare et al. (2014; Fig. 9). This was previously reported by Duparc et al. (2016) for magnetite from Archean felsic intrusions and could reflect the initial composition of the parental magmas.

The nature of the parental magmas (e.g. basaltic, picritic, komatiitic) of the mafic to ultramafic intrusions could affect the chemical composition of magnetite. For example, magnetite from massive sulphides of the Eagle's Nest ultramafic-dominated intrusion has higher concentrations of compatible elements and lower concentrations of incompatible elements than magnetite from the Mayville intrusion (Fig. 4). The Mayville intrusion crystallized from basaltic parental magmas (Yang et al., 2013). In contrast, the Eagle's Nest dyke is associated with a komatiitic parental magma (Mungall et al., 2010; Zuccarelli et al., 2018), resulting from a higher degree of partial melting and, therefore, initially enriched in the most compatible elements and depleted in incompatible elements relative to a basaltic magma. Thus, the trace element contents of the magnetite from the Eagle's Nest dyke suggest that magnetite that crystallizes from an ultramafic parental magma will have a more primitive chemical signature than that which forms from a mafic parental magma.

Influence of the Co-crystallizing Minerals

The nature of the minerals that crystallize with magnetite also affects the minor and trace element composition of Fe-oxides (e.g. Dare et al., 2014). The composition of the magnetite from the Baie Chapus Pyroxenite is a good example of this co-crystallizing effect. The Baie Chapus Pyroxenite is associated with a relatively primitive, mantle-derived parental magma (Sappin et al., 2015a) and the magnetite from this ultramafic-dominated intrusion has a relatively primitive composition, with high Mg and Ni contents and low Al, Ga, and Zn contents (Fig. 2, 3). However, the magnetite also has lower Cr and V contents than expected (Fig. 2, 3). The lower Cr contents could be explained by the fractional crystallization of chromite at depth from this primitive silicate liquid, which would have resulted in a significant decrease in the amount of Cr available in the magma for the Fe-oxides formed later. Furthermore, the low V contents of the magnetite from the pyroxenite relative to that from the semi-massive to massive Fe-Ti oxides of the Baie Chapus Pyroxenite

(Fig. 2, 3, 8c, Table 2) could be explained by the competition for the partitioning of V between magnetite and co-crystallizing clinopyroxene. During magmatic processes, V is strongly partitioned into magnetite ($D_V^{Mag/Silicate\ melt}$ = 26.0: Esperança et al., 1997), but V also has a compatible behaviour with clinopyroxene ($D_V^{Cpx/Basaltic\ melt}$ = 3.1: Hart and Dunn, 1993). The pyroxenite is mainly composed of clinopyroxene with magnetite occurring as an accessory phase, whereas the semi-massive to massive oxide layers are primarily composed of magnetite with minor clinopyroxene. Thus, the high proportion of clinopyroxene in the pyroxenite could explain the depletion in V in magnetite from the ultramafic rocks relative to magnetite from the semi-massive to massive oxide layers.

Fe-Oxide Composition as a Fractionation and Stratigraphic Indicator

Regional scale

The chemical composition of Fe-oxides with respect to compatible and incompatible elements during fractionation processes is a good indicator of the degree of magmatic fractionation of the mafic to ultramafic intrusions in the Superior Province. Based on the magnetite composition of the oxide-bearing mafic to ultramafic rocks and the semi-massive to massive Fe-Ti oxides from the mafic-dominated intrusions, it appears that the Rivière Bell and Lac Doré complexes in the Wawa-Abitibi terrane have the most evolved composition, containing magnetite that is poor in compatible elements and rich in incompatible elements (Fig. 2, 3). The Oxtoby Lake intrusion, located in the Uchi domain, hosts magnetite with intermediate composition of compatible and incompatible elements (Fig. 2). On the other hand, the Croal Lake, Big Mac, Butler, and Highbank-Fishtrap intrusions, in the Oxford-Stull domain, appear to have a more primitive composition, as magnetite from these intrusions are rich in compatible elements (Fig. 2, 3), and magnetite from the Wabassi Main intrusion, in the Uchi domain, shows the most primitive signature of compatible elements (Fig. 2). Its high concentrations of incompatible elements, Al, Mn, and Ti (Fig. 2), could be related to the presence of numerous micro- to nano-scale exsolutions of ilmenite (for Mn and Ti) and Al-spinel (for Al) in the magnetite grains. Indeed, in magnetite from the Wabassi Main intrusion, Al-Mn-Ti contents increase with decreasing Fe contents (EPMA data). Identifying the most primitive and evolved intrusions in the Superior Province may help identify which intrusions in the area are most likely to host Ni-Cu-(PGE) and Fe-Ti-V-P mineralization.

Local scale

In the Big Mac and Baie Chapus intrusions, the chemical composition of magnetite, in terms of compatible and incompatible elements in mafic magmas, shows a strong geographical control that is mostly independent of the lithologies and the proportion of Fe-oxides in the rocks (Fig. 6, 8) and efficiently tracks the magmatic fractionation and indicates the way-up of each intrusion. Magnetite in the northern part of the Big Mac intrusion has a more primitive composition than in the southern area, suggesting that the northern intrusive rocks represent more vent-proximal facies and that the southern rocks are more distal facies. Similarly, the stratigraphic base of the Baie Chapus Pyroxenite appears to be located in the eastern part of the intrusion, as suggested by the occurrence of the most primitive magnetite in this area. These results are also supported by lithofacies distribution, geochemistry, and silicate mineral chemistry. Together these data help to constrain the internal stratigraphy and thus to target the most prospective areas to host Fe-Ti-V mineralization within these intrusions.

Magnetite Composition as an Indicator of the Fe-Ti-V or Fe-Ti-P Prospectivity

The Big Mac mafic intrusion is recognized as an area prospective for Fe-Ti-V mineralization (e.g. Metsaranta and Houlé, 2013; Sappin et al., 2015b; Houlé et al., 2019). In particular, the northern part of this intrusion appears to have the highest potential to host Fe-Ti-V mineralization. The semi-massive to massive oxide layers are restricted to this northern area and show high Fe, Ti, and V contents. In these magnetite-bearing horizons, the best mineralized interval (9.5 m thick) has an average composition of 68 wt% FeO_t, 17 wt% TiO_2, and 0.5 wt% V_2O_5, with a maximum of 76 wt% FeO_t, 19 wt% TiO_2, and 0.6 wt% V_2O_5. Magnetite from the mafic and ultramafic rocks and the semi-massive to massive Fe-Ti oxide layers in the northernmost area also have the most primitive composition, with high V contents (8653–1653), a composition favourable to the formation of Fe-Ti-V deposits. In addition, based on the Ni+Cr versus Ti+V discrimination diagram, the Ni+Cr values are mostly >400 ppm in magnetite from the intrusive rocks and from the Fe-Ti oxide layers in the northernmost and north-central parts of the Big Mac intrusion and are the same as Ni+Cr values in magnetite from Fe-Ti-V deposits (Fig. 10e,f). In contrast, in the southern area, the semi-massive to massive oxide layers are absent and magnetite from the mafic rocks shows a more evolved composition, with lower V contents (1870–90 ppm). These Fe-oxides also have Ni+Cr contents (<400 ppm) similar to that of more evolved magnetite from Fe-Ti-P deposits, according to the Ni+Cr versus Ti+V diagram (Fig. 10e,f). In

the southernmost part of the intrusion, magnetite is also hosted by rocks rich in apatite, suggesting that this area has more potential for Fe-Ti-P mineralization.

The Baie Chapus Pyroxenite, which is known for its potential to host Fe-Ti-V mineralization, contains semi-massive to massive oxide layers with high Fe, Ti, and V contents (up to 66 wt% Fe_2O_{3t}, 9 wt% TiO_2, and 0.7 wt% V_2O_5: Sappin et al., 2015a). Furthermore, the magnetite from the pyroxenite and the semi-massive to massive Fe-Ti oxide layers has a primitive composition with high V contents (up to 7440 ppm) and Ni+Cr contents similar to magnetite from Fe-Ti-V deposits in the Ni+Cr versus Ti+V diagram (Fig. 10e), confirming the prospectivity of the Baie Chapus Pyroxenite to host Fe-Ti-V mineralization.

These results confirm that the chemical composition of magnetite in mafic to ultramafic intrusions can serve as an indicator of the Fe-Ti-V or Fe-Ti-P prospectivity of these types of intrusions.

Archean Signature of Magnetite?

The EPMA analytical results of magnetite from samples of oxide-bearing mafic to ultramafic rocks and semi-massive to massive Fe-Ti oxides suggest that the magnetite from these rock types may have a distinctive Archean signature. For example, in the Ni/(Cr+Mn) versus Ti+V and Ca+Al+Mn versus Ti+V discrimination diagrams of Dupuis and Beaudoin (2011) and the Ni+Cr versus Ti+V discrimination diagram of Méric (2011), magnetite from the Archean intrusions containing the intrusive rocks and the Fe-Ti oxide layers of this study has significantly lower Ti+V contents than magnetite from the Proterozoic and Phanerozoic Fe-Ti deposits used to construct the diagrams (Fig. 10a,c,e). As can be seen on these discrimination diagrams (Fig 10a,c,e), the Rivière Bell magnetite displays a distinct chemical signature, with higher Ti+V contents, which could be due to ubiquitous fine ilmenite exsolutions in the Fe-oxide grains and/or remobilization of Ti during the greenschist-amphibolite-facies metamorphism that affected the intrusion after its emplacement (Polivchuk, 2017). The dichotomy between the Archean and Proterozoic magnetite composition does not appear to be related to an analytical error, as our Lac Doré magnetite has similar Ti+V values as the Lac Doré magnetite, which was analyzed previously (*see* Fig. 5 and 6 in Dupuis and Beaudoin, 2011). One explanation for this difference could be that there is lower Ti and/or V contents in magnetite from Archean Fe-Ti deposits than from younger deposits.

Another trend visible from the discrimination diagrams is that the LA-ICP-MS data appear better at correctly predicting the deposit type as the Ti contents determined by LA-ICP-MS are often higher than those determined by EPMA. However, a fair amount of the LA-ICP-MS data points still fall into other hydrothermal deposit types, especially data for Ti-poor magnetite from the Oxtoby Lake intrusion and also some data for magnetite from intrusions in the Ring of Fire area (Fig. 10b,d,f).

In the light of all these results, further investigations are needed to better understand which factors control this distinctive Archean signature of magnetite and to constrain the use of discrimination diagrams for magnetite to fingerprint the mineral deposit types, as they appear to be sensitive to other factors than solely the chemical composition of magnetite.

IMPLICATIONS FOR EXPLORATION

The chemical composition of magnetite is useful for determining the degree of fractionation and the internal stratigraphy of the intrusions hosting orthomagmatic mineralization and to identify the areas most prospective for this style of mineralization. Coupled with the fact that Fe-oxides are ubiquitous in mafic to ultramafic rocks and are resistant to mechanical and chemical weathering, magnetite could be used efficiently to gain useful information about the intrusions themselves within structurally deformed and metamorphosed Archean and Proterozoic greenstone belts. Furthermore, even though some of the minor and trace element contents of magnetite can be affected by the presence of exsolutions and/or inclusions, the nature of the parental magmas, or the type of co-crystallizing minerals, on the whole, the composition of this Fe-oxide is independent of the nature of its host rocks. This suggests that it is not necessary to have heavily mineralization samples to identify which unit(s) might be prospective for hosting orthomagmatic mineralization. In particular, the Ni+Cr contents of the magnetite appear to be a very interesting tool for determining the prospectivity of mafic to ultramafic intrusions to host Fe-Ti-V or Fe-Ti-P mineralization, irrespective of the amount of Fe-oxides in the rocks. However, the use of discrimination diagrams to estimate which type of mineralized environment is associated with the magnetite should be undertaken with caution.

ONGOING AND FUTURE WORK

Future research in the context of this project would include the study of ilmenite compositions analyzed by EPMA and LA-ICP-MS and the partial least squares-discriminant analysis (PLS-DA) of the minor and trace element contents of Fe-Ti oxides to confirm our preliminary results regarding the chemical signatures of magnetite from the mafic to ultramafic intrusions in the Superior Province. Comparison of the Fe-Ti oxides data from this study with magnetite and ilmenite compositions from previous work on these intrusions (e.g. Polivchuk, 2017; Arguin et al., 2018) and on other

mafic and ultramafic intrusions in the Superior Province, as well as in other geological provinces, would also help clarify if there is a specific regional signature of these oxides across the Superior. Additional studies are also required to identify the factors controlling the possible Archean-specific signature of Fe-oxides and discuss the applicability of discrimination diagrams to fingerprint Archean magnetite.

ACKNOWLEDGMENTS

This report is a contribution to NRCan's Targeted Geoscience Initiative Program (TGI-5). Support for this study was provided through the Orthomagmatic Ni-Cu-PGE-Cr Ore Systems Project's 'Activity NC-2.2: Ni-Cr metallotect: Synthesis, updates, and revised models for the Superior Province'.

We would like to thank Northern Shield Resources Inc. (C. Vaillancourt, I. Bliss, R.-L. Simard, and G. Budulan), R. Metsaranta from the Ontario Geological Survey (OGS), and V. Bécu from the Geological Survey of Canada (GSC) for providing representative samples. Thanks are also extended to M. Choquette (Université Laval) for his assistance with EPMA analyses, and Z. Yang, D. Petts, and S.E. Jackson (GSC) for their assistance with LA-ICP-MS analyses. This report benefited from the scientific review of Sarah Dare (Université du Québec à Chicoutimi) and Wouter Bleeker (GSC) and editorial review by Elizabeth Ambrose and Valérie Bécu.

REFERENCES

Arguin, J.-P., Pagé, P., Barnes, S.-J., Girard, R., and Duran, C., 2018. An integrated model for ilmenite, Al-spinel, and corundum exsolutions in titanomagnetite from oxide-rich layers of the Lac Doré Complex (Québec, Canada); Minerals, v. 8, 39 p.

Boutroy, E., Dare, S.A.S., Beaudoin, G., Barnes, S.-J., and Lightfoot, P.C., 2014. Magnetite composition in Ni-Cu-PGE deposits worldwide: application to mineral exploration; Journal of Geochemical Exploration, v. 145, p. 64–81.

Dare, S.A.S., Barnes, S.-J., and Beaudoin, G., 2012. Variation in trace element content of magnetite crystallized from a fractionating sulfide liquid, Sudbury, Canada: Implications for provenance discrimination; Geochimica et Cosmochimica Acta, v. 88, p. 27–50.

Dare, S.A.S., Barnes, S.-J., Beaudoin, G., Méric, J., Boutroy, E., and Potvin-Doucet, C., 2014. Trace elements in magnetite as petrogenetic indicators; Mineralium Deposita, v. 49, p. 785–796.

Duparc, Q., Dare, S.A.S., Cousineau, P.A., and Goutier, J., 2016. Magnetite chemistry as a provenance indicator in Archean metamorphosed sedimentary rocks; Journal of Sedimentary Research, v. 86, p. 542–563.

Dupuis, C. and Beaudoin, G., 2011. Discriminant diagrams for iron oxide trace element fingerprinting of mineral deposit types; Mineralium Deposita, v. 46, p. 319–335.

Esperança, S., Carlson, R.W., Shirey, S.B., and Smith, D., 1997. Dating crust-mantle separation: Re-OS isotopic study of mafic xenoliths from central Arizona; Geology, v. 25, p. 651–654.

Hart, S.R. and Dunn, T., 1993. Experimental cpx/melt partitioning of 24 trace elements; Contributions to Mineralogy and Petrology, v. 113, p. 1–8.

Houlé, M.G., Lesher, C.M., McNicoll, V.J., Metsaranta, R.T., Sappin, A.-A., Goutier, J., Bécu, V., Gilbert, H.P., and Yang, X.M., 2015a. Temporal and spatial distribution of magmatic Cr-(PGE), Ni-Cu-(PGE), and Fe-Ti-(V) deposits in the Bird River–Uchi–Oxford-Stull–La Grande Rivière–Eastmain domains: a new metallogenic province within the Superior Craton; *in* Targeted Geoscience Initiative 4: Canadian Nickel-Copper-Platinum Group Elements-Chromium Ore Systems — Fertility, Pathfinders, New and Revised Models, (ed.) D.E. Ames and M.G. Houlé; Geological Survey of Canada, Open File 7856, p. 35–48.

Houlé, M.G., Goutier, J., Sappin, A.-A., and McNicoll, V.J., 2015b. Regional characterization of ultramafic to mafic intrusions in the La Grande Rivière and Eastmain domains, Superior Province, Quebec; *in* Targeted Geoscience Initiative 4: Canadian Nickel-Copper-Platinum Group Elements-Chromium Ore Systems — Fertility, Pathfinders, New and Revised Models, (ed.) D.E. Ames and M.G. Houlé; Geological Survey of Canada, Open File 7856, p. 125–137.

Houlé, M.G., Lesher, C.M., Metsaranta, R.T., and Sappin, A.-A., 2019. Architecture of magmatic conduits in chromium-(PGE) and Ni-Cu-(PGE) ore systems in Superior Province: example from the 'Ring of Fire' region, Ontario; *in* Targeted Geoscience Initiative: 2018 report of activities, (ed.) N. Rogers; Geological Survey of Canada, Open File 8549, p. 441–448.

Houlé, M.G., Lesher, C.M., Sappin, A.-A., Bédard, M.-P., Goutier, J., and Yang, X.M., 2020. Overview of Ni-Cu-(PGE), Cr-(PGE), and Fe-Ti-V magmatic mineralization in the Superior Province: Insights on metallotects and metal endowment; *in* Targeted Geoscience Initiative 5: Advances in the understanding of Canadian Ni-Cu-PGE and Cr ore systems – Examples from the Midcontinent Rift, the Circum-Superior Belt, the Archean Superior Province, and Cordilleran Alaskan-type intrusions, (ed.) W. Bleeker and M.G. Houlé; Geological Survey of Canada, Open File 8722, p. 117–139.

Huang, X.-W., Sappin, A.-A., Boutroy, E., Beaudoin, G., and Makvandi, S., 2019. Trace element composition of igneous and hydrothermal magnetite from porphyry deposits: relationship to deposit subtypes and magmatic affinity; Economic Geology, v. 114, p. 917–952.

Jarosewich, E., Nelen, J.A., and Norberg, J.A., 1980. Reference samples for electron microprobe analysis; Geostandards Newsletter, v. 4, p. 43–47.

Kuzmich, B., 2014. Petrogenesis of the ferrogabbroic intrusions and associated Fe-Ti-V-P mineralization within the McFaulds Lake greenstone belt, Superior Province, northern Ontario, Canada; M.Sc. thesis, Lakehead University, Thunder Bay, Ontario, 486 p.

Maier, W.D., Barnes, S.-J., and Pellet, T., 1996. The economic significance of the Bell River Complex, Abitibi subprovince, Quebec; Canadian Journal of Earth Sciences, v. 33, p. 967–980.

Mathieu, L., 2019. Origin of the vanadiferous serpentine–magnetite rocks of the Mt. Sorcerer area, Lac Doré layered intrusion, Chibougamau, Québec; Geosciences, v. 9, p. 1–36.

Méric, J., 2011. Caractérisation géochimique des magnétites de la zone critique de l'intrusion magmatique de Sept-Îles (Québec, Canada) et intégration à une base de données utilisant la signature géochimique des oxydes de fer comme outil d'exploration; Internship report, Université du Québec à Chicoutimi, Chicoutimi, Quebec, 48 p.

Metsaranta, R.T. and Houlé, M.G., 2013. An update on regional bedrock geology mapping in the McFaulds Lake ("Ring of Fire") region; *in* Summary of Field Work and Other Activities 2013; Ontario Geological Survey, Open File Report 6290, p. 50-1–50-12.

Metsaranta, R.T., Houlé, M.G., McNicoll, V.J., and Kamo, S.L., 2015. Revised geological framework for the McFaulds Lake

greenstone belt, Ontario; *in* Targeted Geoscience Initiative 4: Canadian Nickel-Copper-Platinum Group Elements-Chromium Ore Systems — Fertility, Pathfinders, New and Revised Models, (ed.) D.E. Ames and M.G. Houlé; Geological Survey of Canada, Open File 7856, p. 61–73.

Mortensen, J.K., 1993. U-Pb geochronology of the eastern Abitibi Subprovince. Part 1: Chibougamau – Matagami – Joutel Region; Canadian Journal of Earth Sciences, v. 30, p. 11–28.

Mungall, J.E., Harvey, J.D., Balch, S.J., Azar, B., Atkinson, J., and Hamilton, M.A., 2010. Eagle's Nest: a magmatic Ni-sulfide deposit in the James Bay Lowlands, Ontario, Canada; *in* The Challenge of Finding New Mineral Resources: Global metallogeny, innovative exploration, and new discoveries. Volume II: Zinc-lead, nickel-copper-PGE, and uranium, (ed.) R.J. Goldfarb, E.E. Marsh, and T. Monecke; Society of Economic Geologists, Special Publication 15, p. 539–557.

Ontario Geological Survey–Geological Survey of Canada (OGS-GSC), 2011. Ontario airborne geophysical surveys, gravity gradiometer and magnetic data, grid and profile data (ASCII and Geosoft® formats) and vector data, McFaulds Lake area; Ontario Geological Survey, Geophysical Data Set 1068.

Percival, J.A., Skulski, T., Sanborn-Barrie, M., Stott, G.M., Leclair, A.D., Corkery, M.T., and Boily, M., 2012. Geology and tectonic evolution of the Superior Province, Canada; *in* Tectonic Styles in Canada: The LITHOPROBE Perspective, (ed.) J.A. Percival, F.A. Cook, and R.M. Clowes; Geological Association of Canada, Special Paper 49, p. 321–378.

Polivchuk, M., 2017. The formation of vanadium deposits in the Archean Rivière Bell Complex, Quebec: Insights from Fe-Ti oxide chemistry; M.Sc. thesis, University of Ottawa, Ottawa, Ontario, 146 p.

Sappin, A.-A., Houlé, M.G., Goutier, J., and McNicoll, V., 2015a. Caractérisation pétrographique et géochimique de la Pyroxénite de baie Chapus, Baie-James: Un exemple de minéralisation en Fe-Ti-V dans la Province du Supérieur; Geological Survey of Canada, Open File 7745, 1 sheet.

Sappin, A.-A., Houlé, M.G., Lesher, C.M., Metsaranta, R.T., and McNicoll, V.J., 2015b. Regional characterization of mafic-ultramafic intrusions in the Oxford-Stull and Uchi domains, Superior Province, Ontario; *in* Targeted Geoscience Initiative 4: Canadian Nickel-Copper-Platinum Group Elements-Chromium Ore Systems — Fertility, Pathfinders, New and Revised Models, (ed.) D.E. Ames and M.G. Houlé; Geological Survey of Canada, Open File 7856, p. 75–85.

Sappin, A.-A., Houlé, M.G., Lesher, C.M., McNicoll, V., Vaillancourt, C., and Kamber, B.S., 2016. Age constraints and geochemical evolution of the Neoarchean mafic–ultramafic Wabassi Intrusive Complex in the Miminiska–Fort Hope greenstone belt, Superior Province, Canada; Precambrian Research, v. 286, p. 101–125.

SIGÉOM, 2020. Système d'information géominière du Québec. Ministère de l'Énergie et des Ressources naturelles du Québec. <http://sigeom.mines.gouv.qc.ca> [accessed February 9, 2020]

Stott, G.M., Corkery, M.T., Percival, J.A., Simard, M., and Goutier, J., 2010. A revised terrane subdivision of the Superior Province; *in* Summary of Field Work and Other Activities 2010; Ontario Geological Survey, Open File Report 6260, p. 20-1–20-10.

Yang, X.M., Gilbert, H.P., Houlé, M.G., Bécu, V., McNicoll, V.J., and Corkery, M.T, 2013. The Neoarchean Mayville mafic-ultramafic intrusion in the Bird River greenstone belt, southeastern Manitoba: Geological setting, geochemical variation and the implications for Cu-Ni-PGE-Cr mineral exploration; Geological Association of Canada-Mineralogical Association of Canada, Program with Abstracts, v. 36, p. 200–201.

Zuccarelli, N., Lesher, C.M., and Houlé, M.G., 2018. Sulphide textural variations and multiphase ore emplacement in the Eagle's Nest Ni-Cu-(PGE) deposit, McFaulds Lake greenstone belt, Ontario; *in* Targeted Geoscience Initiative: 2017 report of activities, volume 2, (ed.) N. Rogers; Geological Survey of Canada, Open File 8373, p. 29–34.